

Wafer-Level Thermocompression Bonds

Christine H. Tsau, Martin A. Schmidt, and S. Mark Spearing
Massachusetts Institute of Technology
Cambridge, MA 02139, USA.

Abstract— Thermocompression bonding of gold is a promising technique for achieving low temperature, wafer-level bonding without the application of an electric field or complicated pre-bond cleaning procedure. The presence of a ductile layer influences the fracture behavior of the bonds. The fabrication process was described. In addition, the effect of plasticity was explored by varying the gold bonding thickness between 0.23 to 1.4 μm . Wafers were bonded at 300°C and two different pressures: 1.25 and 7 MPa. The bond toughness of the specimens were characterized using a four-point bend delamination technique. Cohesive failure was found to be the dominant fracture mode in the thicker films. Bonds made with thin gold films failed adhesively and at lower strain energy release rates.

Index Terms— wafer bonding, thermocompression bonding, plasticity

I. INTRODUCTION

Wafer bonding technology has enabled the fabrication of a wide range of micro-fabricated devices, from accelerometers to fluidic systems to chemical reactors [1]. Different bonding techniques are chosen based on the fabrication process and materials involved. For example, high temperature Si fusion bonding forms integral silicon stacks while anodic bonding is suitable for the joining of glass and silicon wafers. The current study focuses on a less common technique called thermocompression bonding, where the simultaneous presence of heat and pressure brings two otherwise separate surfaces together. The fabrication process and technique in which resultant bond toughness was measured are described. Moreover, results of bond toughness as a function of gold bonding layer thickness will be discussed.

A. Thermocompression Bonding

At room temperature, tremendous pressure is required for interatomic attraction to overcome surface asperities [2]. The bondability of the surfaces is enhanced by the application of pressure, and as materials soften with temperature, enables bonding to occur at lower temperatures than

This work was supported by DARPA (F30602-97-C-0127), SRC (2001-MJ-881), SRC Graduate Fellowship.

otherwise possible. This feature is of value in some packaging applications: gold thermocompression is widely used in wire- and die-bonds. Gold is often the material of choice in thermocompression bonding because of its low modulus and oxidation resistant properties. In addition, organics that readily adsorb on the surface can be effectively removed by UV-ozone clean [3]. Few reports involve large area bonding at the wafer-level. Furman and Mita described a process for bonding 127 mm by 127 mm ceramic substrates with up to 60 000 contact pads using a heated press [4]. The minimum pressure of 0.689 MPa was applied for as long as 3 hours, with 1 hour at the peak temperature of either 400 or 375°C and a peak pressure that ranged from 0.689 to 2.76 MPa. These are the pressures that were applied to the substrate. Since the actual bonding area was some fraction of the bond pads, each 150 μm by 450 μm , the actual bonding pressure on the Au was greater than the peak pressure reported. Drost *et al.* reported a pressure of 0.06 MPa at the wafer-level as insufficient for continuous bond formation: bonds were highly localized and on the micrometer scale [5]. Further experiments at the chip-level with varying temperatures showed improvements for pressures up to 1 MPa; further increases in pressure or temperature showed little benefit. However, additional bonding time was found to improve bond homogeneity [5]. Lastly, we have reported wafer-level bonding at 300°C by applying around 1.25 and 7 MPa of pressure on the gold for 10 min [6,7].

B. Four-point bend-delamination

Among the several mechanical testing methods available for characterizing bond toughness, the razor-blade test is often used. As first described by Maszara *et al.*, the toughness of the bond has a fourth order dependency on the measured crack length that resulted from the insertion of a razor blade [8]. In this work, a four-point bend-delamination method is used to assess the bond toughness.

In brittle materials, the toughness is essentially the surface energy. In fracture involving ductile layers, however, additional energy can be dissipated. The toughness of a bond can be quantified by the critical energy release rate,

\mathcal{G}_c . Crack propagation, or bond failure, will not occur until the critical load associated with \mathcal{G}_c is reached. A typical four-point bend specimen is shown in Fig. 1a. By establishing a constant moment condition between the two inner rollers for crack propagation, the resulting strain energy release rate is independent of crack length [9]. The critical strain energy release rate for the specimens studied is defined as:

$$\mathcal{G}_c = \frac{3(1-\nu^2)}{2E} \left(\frac{P_c l}{b} \right)^2 \left(\frac{1}{h_1^3} - \frac{1}{(h_1 + h_2)^3} \right), \quad (1)$$

where E is the Young's modulus, ν is the Poisson's ratio, P_c is the critical load at which crack propagations, l is the distance between the upper and lower rollers, and b is the width of the specimen. The subscripts 1 and 2 refers to un-notched wafer and notched wafer, respectively, as shown in Fig. 1a. As Equation 1 shows, \mathcal{G}_c depends only on the specimen geometry and applied load, both of which can be measured quite accurately.

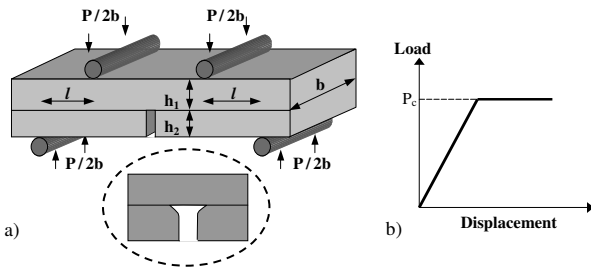


Fig. 1. (a) Illustration of a four-point bend delamination specimen. Inset details the notch region formed by the KOH etch. (b) Ideal load-displacement behavior. P_c is the critical load at which crack propagates and used in \mathcal{G}_c calculations.

II. EXPERIMENTAL PROCEDURE

Each bonding pair consisted of 4" n-type Si wafers with average thicknesses of 525 μm and 450 μm , the latter being a double-side polished (DSP) wafer. The notch geometry shown in Fig. 1a was formed by KOH etching a 500 μm wide and 60 μm deep central trench in the DSP wafer. To prevent resist pull back near the trench edges, a 100 μm wide and less than 1 μm deep feature was isotropically etched around the perimeter of the central trench. Approximately 3000 \AA of thermal oxide was then grown on both wafers. Next, wafers were patterned using AZ5214E image reversal resist in preparation for e-beam deposition of 10 nm Ti adhesion layer and 0.11 to 0.7 μm Au. Lift-off resulted in several 60 mm long lines of constant widths and spacings. The geometries examined were 6 mm and 50 μm wide lines. The lines in the

latter case were spaced 250 μm apart. To ensure complete removal of organics, wafers were UV-ozone cleaned immediately before wafer alignment. Three triangular separators, about 100 μm thick and 1 cm long, were inserted between the wafers at the edges to maintain a vertical separation between wafers until bonding. Bonds were made in an Electronic Visions AB1-PV bonder under a nitrogen atmosphere. Following the temperature ramp and the 3-minute stabilization period at 300°C, 0.02 MPa of pressure was applied and the separators were withdrawn. A bonding pressure of 0.5 MPa was then applied across the wafer for 10 minutes. This bonding pressure corresponding to approximately 1.25 and 7 MPa of pressure on the Au for geometries with 6 mm and 50 μm lines, respectively. The temperature was ramped down subsequently. Highlights of the fabrication process are shown in Fig. 2.

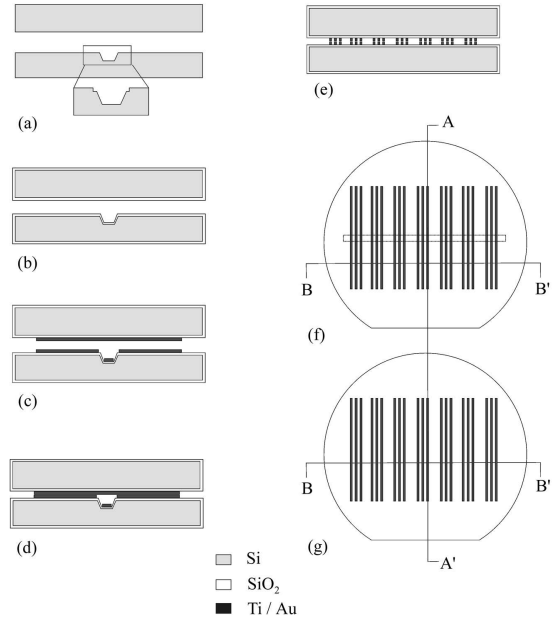


Fig. 2. Schematic of process flow, with cross sections taken along A-A' for (a)-(d), and along B-B' for (e). (a) Bonding pair. Detail shows notch region in DSP wafer (bottom) after KOH and shallow anisotropic etching. (b) Thermal oxidation. (c) Metal deposition. (d),(e) Aligned bonding. (f),(g) Top view of DSP and regular wafers after lift-off, respectively. Dashed central rectangle in (f) indicates the location of the etched trench.

Mechanical test specimens were made by dicing the bonded wafers into 8 mm wide strips. A width-wise cut was made above the KOH-etched notch to the double side polished wafer, exposing the bonded interface, as illustrated in Fig. 1a. Mechanical tests were performed using a servo-hydraulic mechanical testing machine in displacement-controlled mode at a rate of 0.15 mm/min. Load and cross-head displacement data were captured by a LabVIEW program. Real-time observations of the spec-

imen were made with a long working distance microscope. The specimen rested on the outer rollers, which sat on a fixture that was rigidly attached to the upward moving crosshead. The inner rollers were attached to the stationary portion of the testing machine via an adjustable grip located above. The adjustable grip improved the positional leveling of top apparatus. The alignment of the apparatus was checked immediately prior to testing with strain gages located below the inner rollers.

The fracture surface of delaminated specimens were studied. The distance of the crack tip was noted and a width-wise line scribed on the wafer surface. The specimen was then loaded in a 3-point bending jig to promote crack growth from the wafer surface to the interface. It is assumed that the operation introduced no damage to the mating surfaces, since the pieces separated easily with slight applied pressure. Optical microscopy and scanning electron microscopy (SEM) were used to examine the surfaces. The actual bonded area were also measured in the SEM to account for any misalignment during bonding. The toughness values reported here reflect the actual bonded area.

III. RESULTS AND DISCUSSION

A. Fabrication Process

Initially, bonds were made with unoxidized wafers [6]. Discoloration of gold was observed on portions of the wafers that failed to bond. Using Auger spectroscopy, the elemental composition in those regions was identified as silicon with varying amounts of oxygen. The oxygen signal came from oxidation of silicon at the surface. Moreover, sputtering in the Auger showed that the signal intensity of the silicon decreased with distance into the gold. Experiments using a Ge substrate indicated that the silicon had originated from the substrate and had diffused through the gold layer. While the eutectic temperature is 363°C, the interdiffusion of silicon and gold occurs at significantly lower temperatures. Si was observed to accumulate on the gold surface below 340°C [10]. Although the thin film stack included a Ti adhesion layer, no trace of Ti was detected despite the fact that the bonding temperature exceeded the reaction temperature of Ti and Au, which is around 200°C [11], [12]. With only 10 nm of Ti, it is possible that the Ti had completely reacted with either Au or Si (titanium silicides are relatively easy to form as well), preventing elemental Ti from diffusing through the Au layer. The presence of Si at the Au bonding surface will prevent bonding because Si hardens gold, which hampers the thermocompression process. A diffusion barrier layer is thus needed. Silicon dioxide was chosen and a series of diffusion experiments were performed. Thermal oxides of

varying thickness were grown, followed by standard photolithography and metal deposition processes. Annealing at 300°C was carried out in a tube furnace under nitrogen, in order to duplicate the bonding conditions. Concentration of Si was obtained by multiplexing scans around the Au₃ and Si₂ Auger electron energy peaks. After 10 cycles of such scans, the ratio of the counts were taken. Table I shows that an oxide thickness above 1500 Å was sufficient to bar Si from reaching the surface. For the bonding experiments reported here, around 3000 Å thick oxides were used.

TABLE I
CONCENTRATION OF SI WITH VARYING SiO₂ THICKNESS

Anneal time [min]	SiO ₂ thickness [Å]	Si [%]	Note
10	0	35	Post 2 sputter cycles
10	480	6	
10	1550	--	
10	3030	--	
30	3030	--	
60	3030	--	

The KOH etch step described in the process flow was necessitated by the mechanical testing procedure. As described by Charalambides *et al.*, the test specimen has a notch placed in one of the substrates so that the interface is exposed and the crack propagates along the interface. However, the thin interface of the current specimen requires dicing with micrometer scale precision across the wafer. One alternative is to place the notch to within tens of microns of the interface, and then to load the specimen in a three point bending fixture to produce a precrack that runs through the remaining ligament in the DSP wafer, and even a short distance along the interface. To confine the precrack direction and to reduce mechanical interlocking during testing, two cuts were made at the notch: a deep, wide cut of approximately 220 μm in width, followed by a 30 μm wide cut that stops approximately 30 μm away from the bond interface [6]. However, as illustrated in Fig. 3a, the pre-cracks were not always straight, resulting in mechanical interlocking during loading. The low toughness of the bond and the consequently low applied loads makes such interlocking a significant source of error. By implementing the KOH etch, the precracking step and resulting interlocking could be eliminated. The interface is exposed once the notch cut meets the bottom

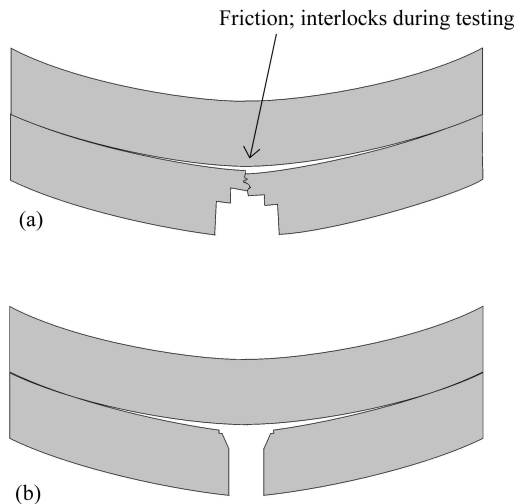


Fig. 3. Schematic of bending specimen in near notch region. (a) Notch made by successive diesaw cuts and 3 point bending to induce a precrack. (b) Notch made by KOH etch. Possibility of mechanical interlocking during loading is eliminated.

of the etched feature.

B. Bond Toughness Results

As mentioned, the critical strain energy release rate of a ductile bond consists of elastic and plastic components. The elastic part is basically the work of adhesion in the absence of any plastic dissipation. Studies of other material systems by other investigators have found that the measured toughness in ductile bonds is a strong function of the thickness of the adhesive layer [13, 14]. A thinner adhesive layer is more severely constrained, which limits the plastic dissipation. The bond layer thickness range examined in this study was rather narrow – ranged from 0.23 to 1.4 μm – therefore \mathcal{G}_c did not exhibit a strong functional dependence on the bond layer thickness in Fig. 4. For specimens with bonding layer thickness greater than 0.52 μm , \mathcal{G}_c ranges from 38 to 66 J/m^2 . Such high \mathcal{G}_c values corresponded to a thin film dielectric stack surrounded by Cu, whose thickness was greater than 6 μm [13]. The yield strength of Cu was higher than that of Au; hence more plastic dissipation can be expected from Au. More energy can be dissipated when bonds fail cohesively¹. This is consistent with the observation that adhesive failure occurred mainly in bonds formed by thinner films and transitioned into mostly cohesive failures in thicker films.

Although data do not show strong dependence on thickness, for the same Au thickness, however, Fig. 4 shows

¹Cohesive failure refers to failure within the Au bonding layer while adhesive failure refers to failure at the Ti and SiO_2 interface.

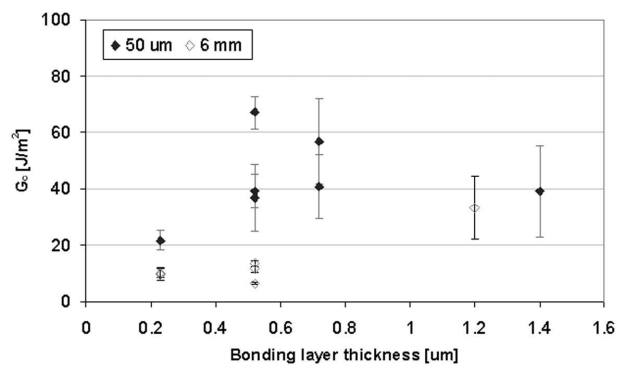


Fig. 4. Critical strain release rate as a function of gold thickness. Each data point represents measurements from 4-7 specimens of the same wafer.

specimens with 6 mm wide Au resulted in lower \mathcal{G}_c values than the ones containing 50 μm lines. By using the same bonding pressure across the wafers in the experiments, the wafers with 50 μm lines experienced a higher bond force on average. Instead of the average 7 MPa applied on the gold, the wafers with 6 mm geometries experienced only around 1.25 MPa. Therefore, it was expected that the specimens with 6 mm lines would result in lower toughness. In addition, specimens with 6 mm wide Au tend to behave more ideally, resembling those found in the purely brittle elastic fracture of Si fusion bonded specimens [15].

The greater scatter associated with higher \mathcal{G}_c is due to plasticity. Higher \mathcal{G}_c is a consequence of plastic energy dissipation, which is sensitive to the extent of local plasticity. A variation in the degree of plasticity was observed, both between specimens and within the same specimen. A scanning electron microscopy (SEM) image of a delaminated specimen is shown in Fig. 5. Fig. 5a. provides a lower magnification view of four delaminated lines, with the crack running in the left-right direction. More deformation was observed in the top two lines of Fig. 5a, where a more clear view could be found in Fig. 5c. Depending on the amount of plasticity, the critical load at which crack propagates would differ, resulting in the relatively large scatter in the \mathcal{G}_c shown. The source of this difference is currently being investigated.

IV. CONCLUSIONS

The bond toughness of Si wafers bonded via gold thermocompression at 300°C under 1.25 and 7 MPa of pressure were characterized using a four-point bend delamination technique. The presence of a thin ductile layer modifies the fracture behavior of an otherwise elastic system. The effect of plasticity was observed in the relative narrow

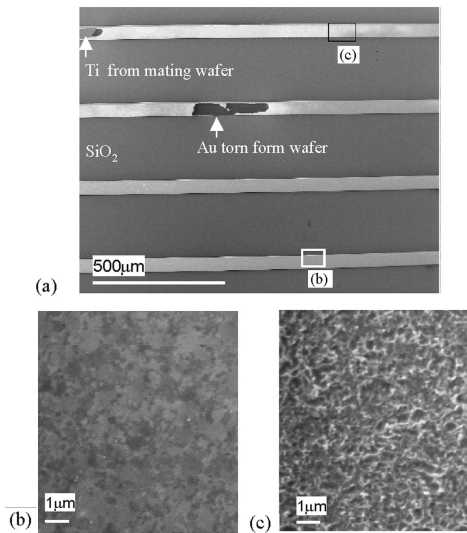


Fig. 5. SEM image of fractured surfaces of a delaminated specimen with bonding layer thickness of $0.72 \mu\text{m}$. (a) Image of 4 lines showing variation in plastic deformation. Bright areas correspond to high plasticity. (b) Higher magnification view of area with low plastic deformation. (c) Higher magnification view of area with high plastic deformation.

range of gold bond layer thickness of 0.23 to $1.4 \mu\text{m}$. The load-displacement curve of specimens bonded with thinner and wider linewidth (6 mm) gold exhibits near-ideal elastic fracture characteristics. Adhesive failure dominated in those specimens. Failure became more cohesive as film thickness increased, consistent with findings by other investigators in other materials systems. Plasticity was found to be sensitive to local variations within the specimen. Unaccounted for process variations probably contributed to the differences in average \mathcal{G}_c between wafers that went through nominally similar process conditions.

V. ACKNOWLEDGEMENTS

The authors would like to acknowledge support from Singapore-MIT Alliance (SMA MOU 11/6/98). Fabrication was carried out at MIT Microsystems Technology Laboratories and tested at MIT Technology Laboratory for Advanced Composites. The authors would like to thank K. Turner for his valuable assistance with the four-point bend setup.

REFERENCES

- [1] M. A. Schmidt, "Wafer-to-wafer bonding for microstructure formation," *Proceedings of the IEEE*, vol. 86, pp. 1575-1585, 1998.
- [2] R. F. Tylecote, *The solid phase welding of metals*. New York: St. Martin's Press, 1968.
- [3] J. L. Jellison, "Effect of surface contamination on the thermocompression bondability of gold," *IEEE Trans. Parts, Hybrids Packag.*, vol. PHP-11, pp. 206-211, 1975.
- [4] B. K. Furman and S. G. Mita, "Gold-Gold (Au-Au) thermocompression (TC) bonding of very large arrays," *Proc. of 42nd Electronic Components and Technology Conference*, 1992, pp. 883-889.
- [5] A. Drost, G. Klink, S. Scherbaum, and M. Feil, "Simultaneous fabrication of dielectric and electrical joints by wafer bonding," *Proc. of SPIE – Micromachined Devices and Components IV*, 1998, pp. 62-71.
- [6] C. H. Tsau, M. A. Schmidt, and S. M. Spearing, "Characterization of low temperature, wafer-level gold-gold thermocompression bonds," *Proc. of Materials Science of Microelectromechanical Systems (MEMS) Devices II*, 1999, pp. 171-176.
- [7] C.H. Tsau, M.A. Schmidt, and S.M. Spearing, "Fabrication Process and Plasticity of Gold-Gold Thermocompression Bonds." *Proc. of the 6th International Symposium on Semiconductor Wafer Bonding: Science, Technology, and Applications*, ECS, 2001.
- [8] W. P. Maszara, G. Goetz, A. Caviglia, and J. B. McKittrick, "Bonding of silicon wafers for silicon-on-insulator," *J. Appl. Phys.*, vol. 64, pp. 4943-4950, 1988.
- [9] P. G. Charalambides, J. Lund, A. G. Evans, and R. M. McMeeking, "A test specimen for determining the fracture resistance of bimaterial interfaces," *J. Appl. Mech.*, vol. 56, pp. 77-82, 1989.
- [10] K. Nakashima, M. Iwami, and A. Hiraki, "Low temperature diffusion of Au into Si in the Si(substrate)-Au(film) system," *Thin Solid Films*, vol. 25, pp. 423-430, 1975.
- [11] H. Hieber, "Aging properties of gold layers with different adhesion layers," *Thin Solid Films*, vol. 37, pp. 335-343, 1976.
- [12] K. Masahiro and S. Noboru, "Effects of temperature, thickness and atmosphere on mixing in Au-Ti bilayer thin films," *J. Materials Science*, vol. 28, pp. 5088-5091, 1993.
- [13] M. Lane, R. H. Dauskardt, A. Vainchtein, and H. Gao, "Plasticity contributions to interface adhesion in thin-film interconnect structures," *J. Mater. Res.*, vol. 15, pp. 2758-2769, 2000.
- [14] I. E. Reimanis, B. J. Dalgleish, and A. G. Evans, "The fracture resistance of a model metal/ceramic interface," *Acta Metall. Mater.*, vol. 39, pp. 3133-3141, 1991.
- [15] K. T. Turner, A. A. Ayon, D. Choi, B. Miller, and S. M. Spearing, "Characterization of silicon fusion bonds using a four-point bend specimen," *Proc. of Materials Science of Microelectromechanical Systems (MEMS) Devices III*, pp. EE6.3.1, 2000.